

A STRONG ELECTROWEAK SECTOR AT FUTURE LINEAR COLLIDERS: COMPARISON OF MODELS

R. Casalbuoni ^{a,b)}, A. Deandrea ^{c)}, S. De Curtis ^{b)}
D. Dominici ^{a,b)}, R. Gatto ^{d)}

a) Dipartimento di Fisica, Univ. di Firenze, I-50125 Firenze, Italia.

b) I.N.F.N., Sezione di Firenze, I-50125 Firenze, Italia.

c) Centre de Phys. Théorique, CNRS, Luminy, Case 907, F-13288 Marseille Cedex 9, France.

d) Dépt. de Phys. Théorique, Univ. de Genève, CH-1211 Genève 4, Suisse.

1 Introduction

In this work we have studied the phenomenological properties at future e^+e^- linear colliders of two models of strong electroweak symmetry breaking, characterized by the presence of new spin one strong interacting resonances.

The first model we have considered is the so called BESS model [1]. This is an effective lagrangian parameterization of the symmetry breaking mechanism, based on a symmetry $G = SU(2)_L \times SU(2)_R$ broken down to $SU(2)_{L+R}$. New vector particles are introduced as gauge bosons associated to a hidden $H' = SU(2)_V$. The symmetry group of the theory becomes $G' = G \otimes H'$. It breaks down spontaneously to $H_D = SU(2)$, which is the diagonal subgroup of G' . This gives rise to six Goldstone bosons. Three are absorbed by the new vector particles while the other three give mass to the SM gauge bosons, after the gauging of the subgroup $SU(2)_L \otimes U(1)_Y \subset G$. The general procedure for building models with vector and axial vector resonances is discussed in [2].

The parameters of the BESS model are the mass of these new bosons M_V , their self coupling g'' , and a third parameter b whose strength characterizes the direct couplings of the new vectors V to the fermions. However due to the mixing of the V bosons with W and Z , the new particles are coupled to

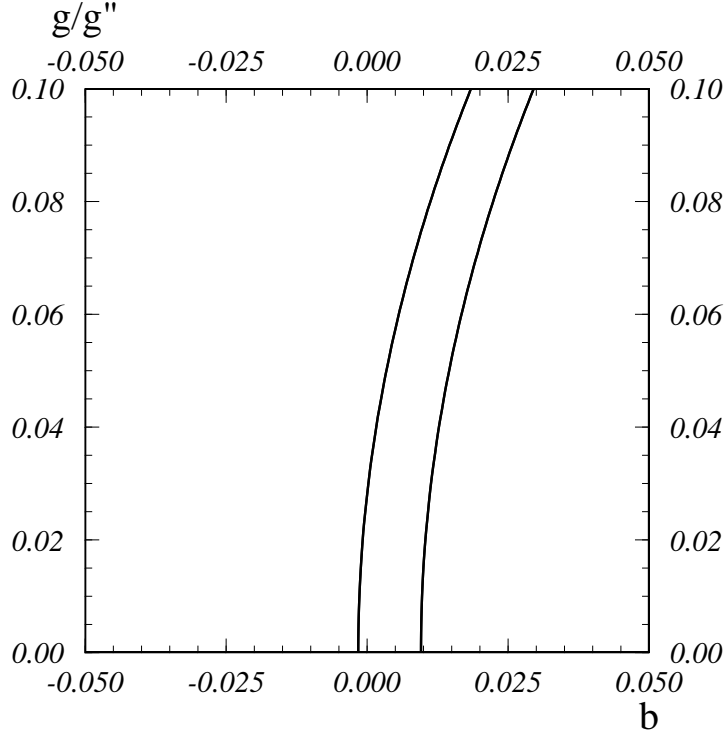


Fig. 1 - BESS model 90% C.L. contour on the plane $(b, g/g'')$ obtained by comparing the theoretical predictions to the experimental data. The allowed region is between the curves.

the fermions also when $b = 0$. The parameter g'' is expected to be large due to the fact that these new gauge bosons are thought of as bound states from a strongly interacting electroweak sector. By taking the formal $b \rightarrow 0$ and $g'' \rightarrow \infty$ limits, the new bosons decouple and the standard model (SM) is recovered. By considering only the limit $M_V \rightarrow \infty$ they do not decouple.

The already existing data (LEP, CDF, SLC, etc.) allow us to get bounds on the parameter space $(b, g/g'')$, as shown in Fig. 1. The bounds do not depend on the mass M_V at least for values above $\approx 300 \text{ GeV}$.

The second model is an extension of the previous one. It is called degenerate BESS model [3]. We start again from the global symmetry group of the theory $G = SU(2)_L \otimes SU(2)_R$, spontaneously broken to $SU(2)_{L+R}$. The new

vector and axial vector bosons correspond to the gauge bosons associated to a hidden symmetry, $H' = SU(2)_L \otimes SU(2)_R$. The symmetry group of the theory becomes $G' = G \otimes H'$. It breaks down spontaneously to H_D (the same as in BESS) and this gives rise to nine Goldstones. Six of these are absorbed by the vector and axial vector bosons, and the other three give masses to the SM gauge bosons. The model includes two new triplets of vector particles (L^\pm , L_3 , R^\pm , R_3). The parameters of the model are a new gauge coupling constant g'' and a mass parameter M , which is the common mass of all the new vector and axial-vector particles, when we neglect the electroweak corrections. Contrarily to the BESS model, in this case we have decoupling in the limit $M \rightarrow \infty$. In the charged sector the fields R^\pm are unmixed for any value of g'' , and therefore they are not coupled to fermions.

The actual data give the bounds in the plane $(M, g/g'')$ illustrated in Fig. 2.

2 Tests at e^+e^- future colliders

In presence of new vector resonances the annihilation channels $e^+e^- \rightarrow f\bar{f}$, and $e^+e^- \rightarrow W^+W^-$ are much more efficient than the fusion channels because all the center of mass energy is used to produce the new particles. For the BESS model, since the new vector particles are strongly coupled, the channel W^+W^- is the dominant one [4]. On the other hand, for the degenerate BESS model, due to its decoupling properties, the W^+W^- channel gets depressed, and the dominant one is $f\bar{f}$ [3].

Our analysis, in the fermion channels, is based on the following observables: the total hadronic and muonic cross sections, the forward-backward asymmetries in muons and $\bar{b}b$ and, assuming a longitudinal polarization P_e of the electron beam, the left-right asymmetries in muons, $\bar{b}b$ and hadrons

$$\sigma^\mu, \quad \sigma^h \tag{1}$$

$$A_{FB}^{e^+e^- \rightarrow \mu^+\mu^-}, \quad A_{FB}^{e^+e^- \rightarrow \bar{b}b} \tag{2}$$

$$A_{LR}^{e^+e^- \rightarrow \mu^+\mu^-}, \quad A_{LR}^{e^+e^- \rightarrow \bar{b}b}, \quad A_{LR}^{e^+e^- \rightarrow had} \tag{3}$$

We have assumed for σ^h (σ^μ) a total error of 2% (1.3%) [3]. For the other observable quantities we assumed only statistical errors.

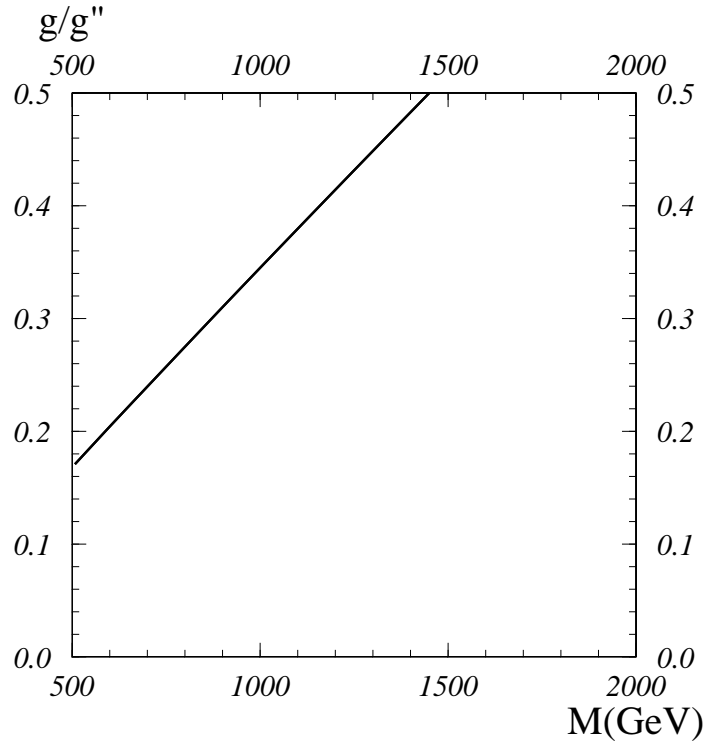


Fig. 2 - *Degenerate BESS model 90% C.L. contour on the plane $(M, g/g'')$ obtained by comparing the theoretical predictions to the experimental data. The allowed region is below the curve.*

Concerning the WW channel, we studied the following observables:

$$\frac{d\sigma}{d\cos\theta}(e^+e^- \rightarrow W^+W^-), \quad A_{LR}^{e^+e^- \rightarrow W^+W^-} \quad (4)$$

where θ is the center of mass scattering angle. We also considered the possibility of measuring the final W polarization by using the W decay distributions, and we added to our observables the longitudinal and transverse polarized W differential cross sections and asymmetries.

In order to get a clear signal for W polarization reconstruction we studied the channel for one W decaying leptonically and the other hadronically. We assumed an effective branching ratio $B = 0.1$ to take into account the loss of luminosity from beamstrahlung [5].

The analysis was performed by taking 19 bins in the angular region restricted by $|\cos\theta| < 0.95$ and assuming systematic errors $\delta B/B = 0.005$, $\delta\mathcal{L}/\mathcal{L} = 1\%$ for the luminosity and 1% for the acceptance.

The machine options we considered are center of mass energies of 360, 500, 800 and 1000 GeV , and corresponding integrated luminosities of 10, 20, 50 and 80 fb^{-1} .

The results for the BESS model are shown in Fig. 3, where the regions in the parameter space (M_V, Γ_V) which can be probed at $\sqrt{s} = 360$ GeV , $L = 10$ fb^{-1} (dashed), $\sqrt{s} = 500$ GeV , $L = 20$ fb^{-1} (continuous) and $\sqrt{s} = 800$ GeV , $L = 50$ fb^{-1} (dot-dashed) by measuring $W_{L,T}W_{L,T}$ differential cross sections and left-right asymmetries are illustrated. The lower narrow solid line is the limit from LEP measurements. The upper narrow solid line is obtained by considering the deviation with respect to the SM prediction and assuming the LEP errors for the corresponding observables.

For instance for $\sqrt{s} = 500$ GeV , one is sensitive for $M_V = 2$ TeV to $\Gamma_V \geq 250$ GeV , for $M_V = 1.5$ TeV to $\Gamma_V \geq 60$ GeV , in agreement with Barklow results [6].

In conclusion measurements of cross sections with different final W polarizations at a linear collider (LC) with $\sqrt{s} = 500$ GeV improve LEP bound up to $M_V \sim 800$ GeV . At $\sqrt{s} = 800$ GeV the sensitivity exceeds the LEPI bound for all values of M_V .

The comparison between LHC and LC is shown in Fig. 4 (5) in the plane $(b, g/g'')$ for a LC of $\sqrt{s} = 500$ GeV and $L = 20$ fb^{-1} assuming $M_V = 1$ TeV ($M_V = 1.5$ TeV). The dotted line corresponds to the 90% C.L. bound from the WW differential cross section, the dashed line to the bound from $W_L W_L$

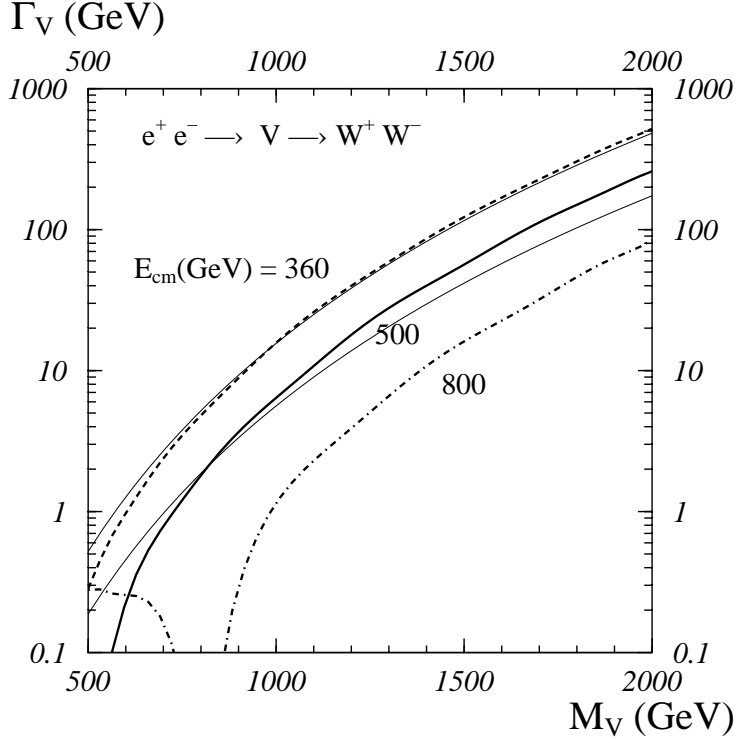


Fig. 3 - BESS model 90% C.L. contour in the (M_V, Γ_V) plane from measurements of differential cross sections and left-right asymmetries; W polarizations are reconstructed from the decay lepton and quark jets. Energy and integrated luminosity are the following: $\sqrt{s} = 360$ GeV, $L = 10 \text{ fb}^{-1}$ (dashed) $\sqrt{s} = 500$ GeV, $L = 20 \text{ fb}^{-1}$ (solid) and $\sqrt{s} = 800$ GeV, $L = 80 \text{ fb}^{-1}$ (dash-dotted). The lower narrow solid line is the limit from LEP measurements. The upper narrow solid line is obtained by considering the deviation with respect to the SM prediction and assuming the LEP errors for the corresponding observables. The allowed region is below the curves.

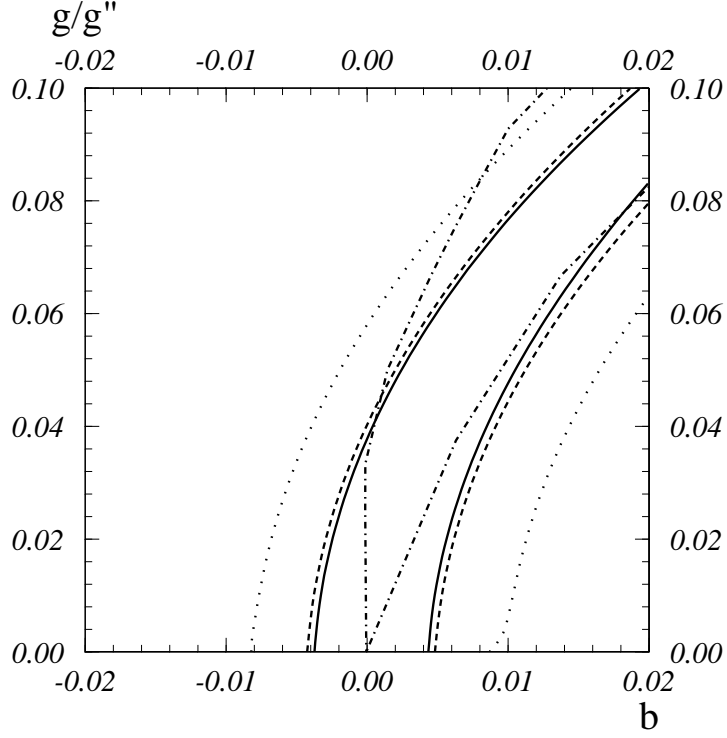


Fig. 4 - BESS model 90% C.L. contours in the plane $(b, g/g'')$ for $M_V = 1$ TeV. The dotted line corresponds to the bound from the WW differential cross section, the dashed line from $W_L W_L$ differential cross sections and the continuous line from the differential $W_{L,T} W_{L,T}$ cross sections and WW left-right asymmetries at a 500 GeV LC. The dot-dashed line corresponds to the bound from the total cross section $pp \rightarrow W^\pm, V^\pm \rightarrow W^\pm Z$ at LHC. The allowed regions are the internal ones.

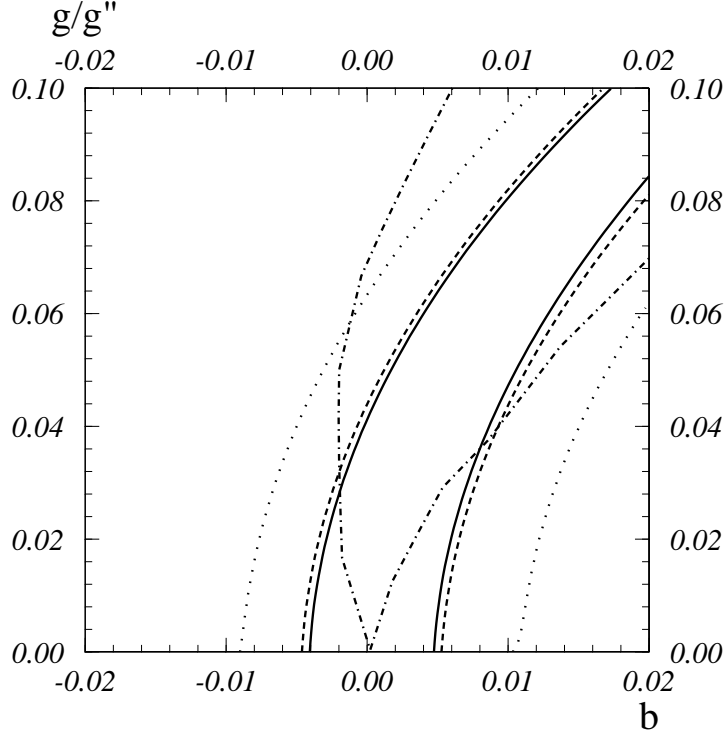


Fig. 5 - BESS model 90% C.L. contours in the plane $(b, g/g'')$ for $M_V = 1.5$ TeV. The dotted line corresponds to the bound from the WW differential cross section, the dashed line from $W_L W_L$ differential cross sections and the continuous line from the differential $W_{L,T} W_{L,T}$ cross sections and WW left-right asymmetries at a 500 GeV LC. The dot-dashed line corresponds to the bound from the total cross section $pp \rightarrow W^\pm, V^\pm \rightarrow W^\pm Z$ at LHC. The allowed regions are the internal ones.

differential cross sections, and the continuous line to the bound combining the differential $W_{L,T}W_{L,T}$ cross sections and WW left-right asymmetries. The dot-dashed line represents the bound from LHC. The allowed regions are the ones between the lines. The bound from LHC is obtained by considering the total cross section $pp \rightarrow W^\pm, V^\pm \rightarrow W^\pm Z \rightarrow \mu\nu\mu^+\mu^-$ and assuming that no deviation is observed with respect to the SM within the experimental error. Statistical and systematic errors of 5% have been assumed.

This is for LHC the more efficient channel for the case of a vector resonance strongly coupled to longitudinal W . LHC can discover such vector resonances in a large region of the parameter space up to masses $M_V = 1.5 - 2 \text{ TeV}$ in the channel $pp \rightarrow W^\pm, V^\pm \rightarrow W^\pm Z$ [7, 8, 9, 10].

In Fig.6, 90% C.L. contours in the plane $(b, g/g'')$ for $M_V = 2 \text{ TeV}$ are shown. The dotted line corresponds to the bound from the WW differential cross section, the dashed line from $W_L W_L$ differential cross sections, and the continuous line from the differential $W_{L,T}W_{L,T}$ cross sections and WW left-right asymmetries at a LC of $\sqrt{s} = 800 \text{ GeV}$ and $L = 50 \text{ fb}^{-1}$. The dot-dashed line corresponds to the bound from the total cross section $pp \rightarrow W^\pm, V^\pm \rightarrow W^\pm Z$ at LHC.

The neutral channel $pp \rightarrow \gamma, Z, V \rightarrow W^+W^-$ suffers of background from $t\bar{t}$ production. Nevertheless the new neutral vector bosons can be studied at LHC, by considering their lepton decays, up to masses of the order of 1 TeV [11]. Notice that while LHC is more sensitive to the charged new vector bosons, the LC is sensitive to the neutral ones (at least in the annihilation channels).

As a general conclusion it seems that for models of new strong interacting vector resonances, if one is able to reconstruct the final W polarization, the measurement of polarized $e^+e^- \rightarrow W_L W_L$ gives rather strong bounds on the parameter space of the model.

Concerning the model with vector and axial-vector resonances degenerate in mass, LHC is sensitive to the new particles in the channels $pp \rightarrow W^\pm, L^\pm \rightarrow \mu\nu$ and $pp \rightarrow \gamma, Z, L_3, R_3 \rightarrow \mu^+\mu^-$ up to masses of the order of 2 TeV as shown in Fig. 7.

The bounds are obtained by assuming no deviations with respect to the SM in the total cross section $pp \rightarrow W^\pm, L^\pm \rightarrow \mu\nu$ within the experimental errors [3]. Statistical and systematic errors of 5% have been assumed. The bounds have to be compared with those coming from LC's in Fig.7. The double dot-dashed line represents the limit from the combined unpolarized

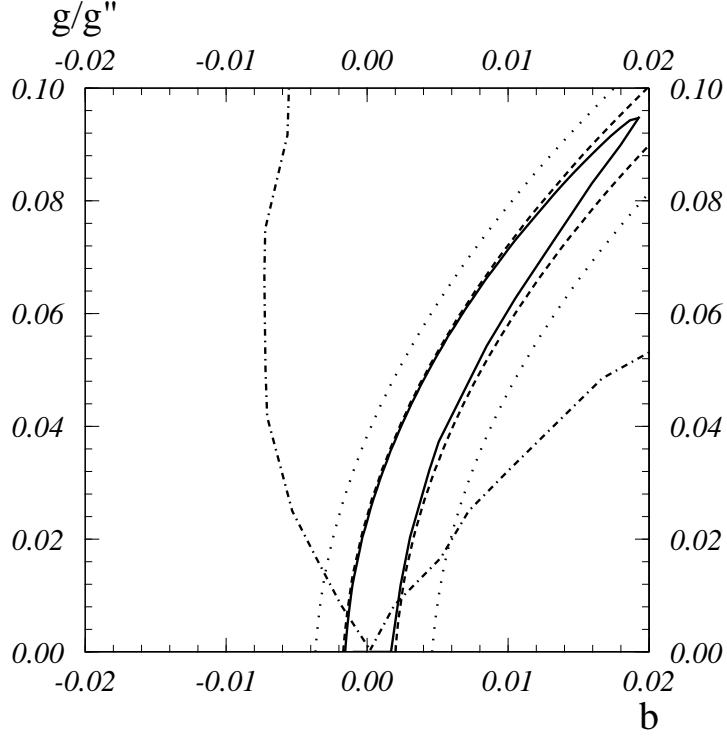


Fig. 6 - BESS model 90% C.L. contours in the plane $(b, g/g'')$ for $M_V = 2 \text{ TeV}$. The dotted line corresponds to the bound from the WW differential cross section, the dashed line from $W_L W_L$ differential cross sections and the continuous line from the differential $W_{L,T} W_{L,T}$ cross sections and WW left-right asymmetries at a 800 GeV LC. The dot-dashed line corresponds to the bound from the total cross section $pp \rightarrow W^\pm, V^\pm \rightarrow W^\pm Z$ at LHC. The allowed regions are the internal ones.

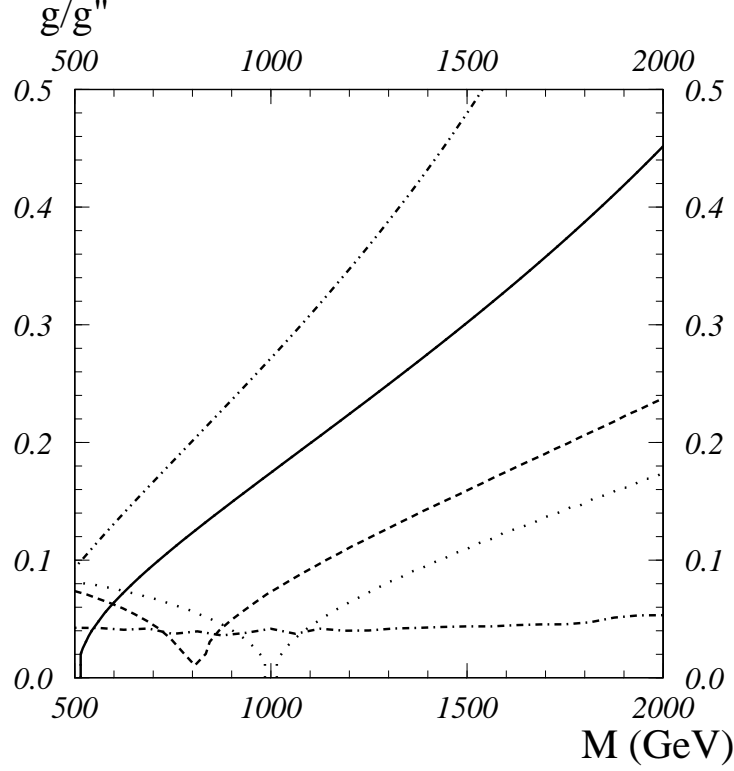


Fig. 7 - Degenerate BESS model 90% C.L. contour on the plane $(M, g/g'')$ from e^+e^- at different \sqrt{s} values: the dash-double-dotted line represents the limit from the combined unpolarized observables at $\sqrt{s} = 360$ GeV with an integrated luminosity of $L = 10 \text{ fb}^{-1}$, the continuous line at $\sqrt{s} = 500$ GeV and $L = 20 \text{ fb}^{-1}$, the dashed line at $\sqrt{s} = 800$ GeV and $L = 50 \text{ fb}^{-1}$, the dotted line at $\sqrt{s} = 1000$ GeV and $L = 80 \text{ fb}^{-1}$. The dot-dashed line represents the limit from LHC. The allowed regions are below the curves.

observables at $\sqrt{s} = 360 \text{ GeV}$ with an integrated luminosity of $L = 10 \text{ fb}^{-1}$; the continuous line from $\sqrt{s} = 500 \text{ GeV}$ and $L = 20 \text{ fb}^{-1}$, the dashed line from $\sqrt{s} = 800 \text{ GeV}$ and $L = 50 \text{ fb}^{-1}$ and the dotted line from $\sqrt{s} = 1000 \text{ GeV}$ $L = 80 \text{ fb}^{-1}$. The dot-dashed line represents the limit from LHC. Therefore, in the case of degenerate BESS, to be competitive with LHC, one would need linear colliders of still higher energies than those considered.

3 Conclusions

We have studied tests for a possible strong electroweak sector by making use of two models: BESS, and degenerate BESS.

The importance of degenerate BESS as a model for a possible strong electroweak sector is that it possesses a symmetry which allows it to elude to a high degree the present precision electroweak tests, notably from LEP. In terms of the spin one resonances present in the model this permits their allowed masses to be lower and their fermionic couplings stronger than for ordinary BESS. Both models have charged as well as neutral resonances. For BESS, LC and LHC play complementary roles, in the sense that while LHC is suitable for the discovery of charged resonances, a linear collider is important for the neutral ones. Besides such complementarity, linear colliders in the considered ranges are found to be quantitatively competitive to LHC if the strong electroweak sector is described in terms of ordinary BESS.

The conclusions are different when degenerate BESS is assumed to hold. This is due to the unique features of such a model. In this case LHC seems to be superior for testing the model when compared with the proposed linear colliders at the energies and luminosities considered. Due to more favorable decay rate of the resonances in fermions the conclusion holds not only for the charged states but also for the neutral states, differently than for ordinary BESS.

In view of the different possibilities that can be envisaged for a possible strong electroweak sector, the general conclusion emerges that both LHC and linear colliders will presumably play crucial roles in testing for such a concept as a still viable alternative to other solutions of the electroweak symmetry breaking problem, such as supersymmetry.

ACKNOWLEDGMENTS

This work is part of the EEC project “Tests of electroweak symmetry breaking and future european colliders”, CHRXCT94/0579 (OFES 95.0200). A.D. acknowledges the support of a TMR research fellowship of the European Commission under Contract nr. ERB4001GT955869.

References

- [1] R.Casalbuoni, S.De Curtis, D.Dominici and R.Gatto, Phys. Lett. **B155**, (1985) 95, Nucl. Phys. **B282**, (1987) 235.
- [2] M.Bando, T.Kugo and K.Yamawaki, Phys. Rep. **164** (1988) 217; R.Casalbuoni, S.De Curtis, D.Dominici, F.Feruglio and R.Gatto, Int. Jour. Mod. Phys. **A4**, (1989) 1065.
- [3] R.Casalbuoni, A.Deandrea, S.De Curtis, D.Dominici, F.Feruglio, R.Gatto and M.Grazzini, Phys. Lett. **B349** (1995) 533; R.Casalbuoni, A.Deandrea, S.De Curtis, D.Dominici, R.Gatto and M.Grazzini, Phys. Rev. **D53** (1996) 5201.
- [4] R.Casalbuoni, P.Chiappetta, A.Deandrea, S.De Curtis, D.Dominici, R.Gatto, Z.Phys. **C60** (1993) 315.
- [5] K.Fujii, Proceedings of the 2nd KEK Topical Conference on e^+e^- Collision Physics, KEK, Tsukuba, Japan, November 26-29 1991, published in KEK e^+e^- 1991, 469.
- [6] T.L.Barklow, in R.Orava, P.Eerola, and M.Nordberg, eds. *Physics and Experiments with Linear Colliders*. (World Scientific, Singapore, 1992), p. 423; T.L.Barklow, in Proceedings of the 8th Meeting of Division of Particles and Fields of the APS, Albuquerque, New Mexico, August 2-6, 1994; T.L.Barklow, in A.Miyamoto and Y.Fujii, eds. *Physics and Experiments with Linear Colliders*. (World Scientific, Singapore, 1996), p. 105.
- [7] R.Casalbuoni, P.Chiappetta, S.De Curtis, F.Feruglio, R.Gatto, B.Mele and J.Terron, Phys. Lett. **B249**, (1990) 130; A.Dobado, M.J.Herrero

- and J.Terron, Z. Phys. **C50**, (1991) 205; *ibidem* (1991) 465; J.Barger, S.Dawson and G.Valencia, Nucl. Phys. **B399**, (1993) 364; S.De Curtis, XI Topical Workshop on P-Pbar Collider Physics Abano Terme (Padova), Italy, hep-ph/9610356.
- [8] CMS Collaboration, CERN report CERN/LHCC/94-38.
 - [9] ATLAS Collaboration, CERN report CERN/LHCC/94-43.
 - [10] J.Bagger et al., Phys. Rev. **D49** (1994) 1246; V.Barger et al., Phys. Rev. **D52** (1995) 3878.
 - [11] R.Casalbuoni, P.Chiappetta, M.C.Cousinou, S.De Curtis, F.Feruglio and R.Gatto, Phys. Lett. **B253** (1991) 275, and in *Large Hadron Collider Workshop*, Proceedings of the Workshop, edited by G.Jarlskog and D.Rein, p.731.